Evaluation of the Kinetic Mechanism of *Escherichia coli* Glycinamide Ribonucleotide Transformylase†

Jae Hoon Shim and Stephen J. Benkovic*

Department of Chemistry, 152 Davey Laboratory, The Pennsylvania State University, University Park, Pennsylvania 16802

Received January 30, 1998; Revised Manuscript Received April 8, 1998

ABSTRACT: A kinetic scheme is presented for *Escherichia coli* glycinamide ribonucleotide transformylase (GAR transformylase, EC 2.1.2.2) based on a steady-state and pre-steady-state kinetic analysis of the reaction in both directions employing stopped-flow absorbance and fluorescence spectroscopy. Steady-state parameters showed that k_{cat} for the reverse direction is about 10 times lower than that for the forward direction although the K_m values for formyl dideazafolate and dideazafolate or for glycinamide ribonucleotide and formyl glycinamide ribonucleotide are similar. No pre-steady-state transient was observed in either direction, and the single-turnover rate constant under saturating levels of substrates in each direction was found to be very close to the respective steady-state k_{cat} value. This indicates that steps involving ternary complexes are rate-determining for steady-state turnover in each direction. By conducting the single-turnover reactions under various preincubation and mixing conditions, a random sequential kinetic mechanism was implicated in which the enzyme binds glycinamide ribonucleotide or formyl dideazafolate productively in no obligatory order. The collective data provided a quantitative kinetic scheme to serve as a basis for the analysis of mutations.

Glycinamide ribonucleotide transformylase (GAR transformylase,[1] EC 2.1.2.2) catalyzes the third step of the de novo purine biosynthetic pathway. This enzyme formylates glycinamide ribonucleotide (GAR) using the 10-formyltetrahydrofolate cofactor to make formylglycinamide ribonucleotide (fGAR) (Scheme 1). The GAR transformylase, especially the product of the *Escherichia coli pur*N gene,[2] has been the subject of intensive structural studies owing to its small size (23 241 Da) (*3*, *4*) relative to the human trifunctional enzyme (*5*). An efficient overexpression system in an auxotropic *E. coli* (*pur*N$^-$, *pur*T$^-$) strain was developed recently (*6*) permitting either wild type or mutant enzyme production. Several high-resolution X-ray structures of the *E. coli* GAR transformylase complexed with substrate analogues revealed the identity of amino acid residues important in the binding of substrates and in catalysis (*7*−*9*), consistent with specific and saturation site-directed mutagenesis studies of active site residues implicated in catalytic activity (*6*). The steady-state kinetic mechanism has been elucidated for the murine GAR transformylase and provided a kinetic scheme following an ordered sequential mechanism with the cofactor binding first (*10*).

Scheme 1. GAR transformylase Reaction

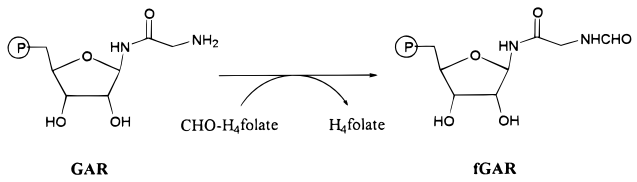

To date no detailed kinetic sequence identifying the rate-determining step has been determined. In this study, we used stopped-flow techniques with *E. coli* GAR transformylase to obtain a detailed kinetic mechanism as a basis for studies of mutant derivatives to define the mechanism of action of the enzyme.

MATERIALS AND METHODS

Materials. β-D-Ribofuranose 1-acetate 2,3,5-tribenzoate, 1-(3-dimethylaminopropyl)-3-ethylcarbodiimide, EDC, bis-(4-nitrophenyl) phosphate, and *N*,*N*-diisopropyl dibenzyl phosphoramidite were purchased from Aldrich and used without purification. *N*-Formylglycine was prepared by the method of Sheehan and Yang (*11*) and recrystallized twice in water. Phosphate assays were performed as described by Chen et al. (*12*). The cofactor 10-formyl-5,8-dideazafolate (fDDF) was purchased from Dr. John Hynes, Medical University of South Carolina, and 5,8-dideazafolate (DDF) was prepared previously in our laboratory by Inglese (*4*). β-Thioglycinamide dideazafolate (β-TGDDF) was synthesized by the procedure of Inglese et al. (*13*). Hydroxyacetamide ribonucleotide (GAROH) was a generous gift from Dr. Dale Boger, The Scripps Research Institute. NMR

† This work was supported by PHS Grant GM24129 from the National Institutes of Health (S.J.B.).

* To whom correspondence should be addressed. Phone: 814-865-2882. Fax: 814-865-2973.

[1] Abbreviations: GAR, β-glycinamide ribonucleotide; GAR transformylase, glycinamide ribonucleotide transformylase; fDDF, 10-formyl-5,8-dideazafolate; DDF, 5,8-dideazafolate; fGAR, formyl-β-glycinamide ribonucleotide; β-TGDDF, β-thioglycinamide dideazafolate; GAROH, β-hydroxyacetamide ribonucleotide; EDC, 1-(3-dimethylaminopropyl)-3-ethylcarbodiimide; DCC, 1,3-dicyclohexylcarbodiimide; BzCl, benzoyl chloride; DMAP, 4-methylaminopyridine; mCPBA, 3-chloroperoxybenzoic acid; TFA, trifluoroacetic acid.

[2] Another GAR transformylase, which is a *pur*T gene product, has been found in *E. coli*. It uses formate and ATP in place of the 10-formyltetrahydrofolate and has been characterized recently (*1*, *2*).

S0006-2960(98)00244-X CCC: $15.00
Published on Web 05/28/1998

spectra were recorded on a Bruker 200, 300, or 360 MHz Spectrometer. HPLC were performed on either a Waters 600E system or a Beckman 421A/110B system. Deuterium oxide (99.9 atom %) was purchased from Aldrich. All kinetics and equilibrium measurements were performed at 25 °C, pH 7.5 in a buffer that contained 50 mM 2-(*N*-morpholino)ethanesulfonic acid, 25 mM ethanolamine, 25 mM Tris, and 100 mM sodium chloride (MTEN buffer).

Enzyme. *E. coli* GAR transformylase was prepared as previously described using a pMSW2 vector in MW12 cell (*6*). Aliquots of purified enzyme were stored at −70 °C at 0.1−0.5 mM concentrations in 50 mM Tris-HCl and 1 mM EDTA, pH 7.5. Enzyme solutions at micromolar concentrations are stable at least 24 h at room temperature without loss of activity. The concentration of the purified protein was determined by either an active site titration with β-TGDDF or a BCA assay method according to the protocol provided by the manufacturer (PIERCE). Both methods gave the same result.

Synthesis of GAR. GAR was prepared by the procedure of Boschelli et al. (*14*) with some modifications. The first modification involved the coupling of the ribosylamine and carbobenzyloxyglycine. In this step, ethyl acetate and EDC were used instead of acetone and DCC as reported. The yield was improved to 92% with the α:β isomer ratio as 2:1. The other modification was in the acetonization step. Instead of Dowex-H^+, bis-(4-nitrophenyl) phosphate was used as an acid catalyst to give an 81% yield of acetonide product after 2 h at room temperature. The final product was a mixture of α- and β-anomers with a ratio of 1:1.6, and its structure was identical by ^{1}H NMR, ^{13}C NMR, and mass spectrometer data to that reported in the literature (*15*, *16*). GAR was precipitated as a barium salt for long-term storage. For kinetic studies, GAR was further purified by a Whatman C-18 Partisil ODS-3 HPLC column (1.2 × 45 cm) by using a linear gradient of 0.1% TFA/H_2O to 100% CH_3CN over 50 min with a flow rate of 3 mL/min. The peaks were monitored at 230 nm, and GAR was eluted at 8 min. The concentration of β anomer of GAR was determined by enzymatic turnover in the presence of a 15-fold excess of fDDF.

Synthesis of fGAR (*Scheme 2*). 2,3,5-Tri-*O*-benzoyl-β-D-ribofuranosyl azide (**1**) was synthesized from β-D-ribofuranose 1-acetate 2,3,5-tribenzoate in quantitative yield by the procedure of Boschelli et al. (*14*). To a solution of azide **1** (2.2 g, 4.6 mmol) in MeOH (150 mL) at room temperature was added NaOMe (0.75 g, 14 mmol). After stirring for 1 h, the reaction mixture was neutralized by adding Dowex 50W-X8 (H^+ form) (ca. 1.2 g). Dowex was removed by filtration, and the filtrate was evaporated in vacuo. The residue was dissolved in H_2O (50 mL), and the resulting solution was washed with diethyl ether (2 × 25 mL). The aqueous layer was concentrated to give the triol. The triol was then dissolved in DMF (20 mL) and reacted with dimethoxypropane (15 mL, 120 mmol) and bis-(4-nitrophenyl)phosphate (3.1 g, 9.1 mmol). The resulting yellow solution was stirred for 2 h at room temperature, and the volatiles were evaporated in vacuo. The yellow residue was dissolved in EtOAc (200 mL), and the organic layer was washed with 10% aqueous $NaHCO_3$ (5 × 50 mL) and saturated aqueous NaCl (50 mL). The organic solution was dried (Na_2SO_4), filtered, and concentrated in vacuo. The small amount of reagent left was removed by a short silica gel column (1 × 5 cm, 1/1 EtOAc/Hexanes) to give **2** (0.97 g, 4.5 mmol, 98%) as a colorless oil: ^{1}H NMR ($CDCl_3$) δ 5.54 (s, 1 H), 4.78 (dd, J = 0.9, 6.0 Hz, 1 H), 4.53 (d, J = 6.0 Hz, 1 H), 4.39 (t, J = 4.9 Hz, 1 H), 3.73 (m, 2 H), 2.34 (t, J = 5.7 Hz, 1 H), 1.50 (s, 3 H), 1.32 (s, 3 H).

Scheme 2. Synthesis of fGAR

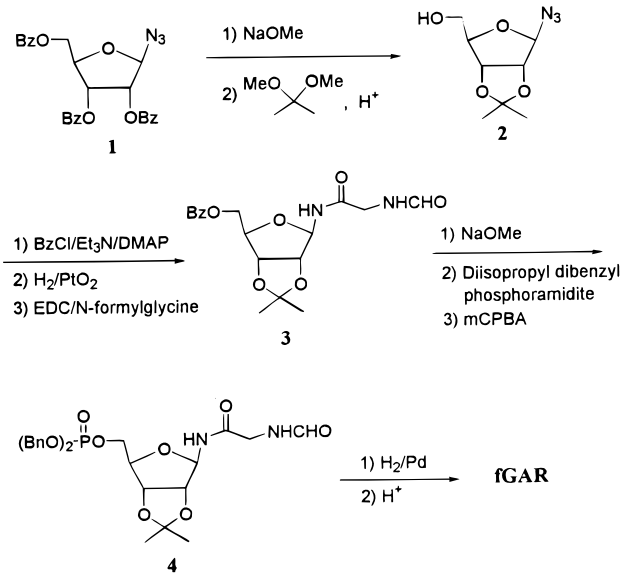

A mixture of azide **2** (0.97 g, 4.5 mmol), BzCl (0.88 mL, 7.5 mmol), Et_3N (1.0 mL, 7.2 mmol), and DMAP (105 mg, 0.88 mmol) in CH_2Cl_2 (50 mL) was stirred at room temperature for 2 h. The solution was diluted with CH_2Cl_2 (50 mL), and the organic layer was washed with H_2O (2 × 50 mL), saturated aqueous $NaHCO_3$ (2 × 50 mL), and saturated aqueous NaCl (50 mL), dried (Na_2SO_4), filtered, and concentrated in vacuo. The resulting yellow oil was dissolved in EtOAc (75 mL) and hydrogenated with PtO_2 (100 mg) under H_2 atmosphere (1 atm). The solution was stirred for 2 h at room temperature. After H_2 was removed by flushing with Ar, $MgSO_4$ (ca. 2 g) was added to the reaction mixture. The resulting suspension was filtered through Celite into a round-bottom flask containing *N*-formylglycine (515 mg, 4.9 mmol) in EtOAc (30 mL). EDC was added (950 mg, 4.9 mmol) to the solution, and the mixture was stirred at room temperature for 12 h. The solution was diluted with EtOAc (75 mL), and the organic layer was washed with H_2O (2 × 50 mL), saturated aqueous $NaHCO_3$ (50 mL), and saturated aqueous NaCl (50 mL), dried (Na_2SO_4), filtered, and concentrated in vacuo. The crude product was purified by a silica gel chromatography (2.5 × 10 cm, EtOAc) to give **3** (680 mg, 1.8 mmol, 40%) as a colorless oil: ^{1}H NMR ($CDCl_3$) δ 8.26 (s, 0.8 H), 8.18 (s, 0.2 H), 8.01 (m, 2 H), 7.53 (m, 3 H), 6.99 (m, 1 H), 6.64 (br s, 1 H), 5.93 (dd, J = 4.1, 9.1 Hz, 0.8 H), 5.60 (d, J = 7.5 Hz, 0.2 H), 4.76 (m, 2 H), 4.53−3.93 (m, 5 H), 1.57 (s, 3 H), 1.35 (s, 3 H).

To a solution of **3** in MeOH (50 mL) was added NaOMe (100 mg, 1.80 mmol). The reaction mixture was stirred for 2 h at room temperature, and MeOH was removed in vacuo. The resulting residue was dissolved in 50% MeOH/$CHCl_3$ (0.2 mL) to load on a short silica gel column (0.5 × 5 cm). The column was washed first with $CHCl_3$ to get rid of methyl benzoate and second with 50% MeOH/$CHCl_3$ to collect

product fractions. The pooled fractions were concentrated to give the debenzoylated intermediate (488 mg, 1.78 mmol, 98%) as a yellow oil: ^{1}H NMR ($CDCl_3$) δ 8.26 (s, 0.8 H), 8.20 (s, 0.2 H), 7.19 (m, 2 H), 5.83 (dd, J = 4.2, 8.9 Hz, 0.8 H), 5.74 (d, J = 7.9 Hz, 0.2 H), 4.74 (m, 2 H), 4.14−3.60 (m, 5 H), 1.53 (s, 3 H), 1.35 (s, 3 H). To a solution of the above intermediate in CH_2Cl_2 (50 mL) at room temperature was added *N*,*N*-diisopropyl dibenzyl phosphoramidite (0.9 mL, 2.7 mmol) and tetrazole (375 mg, 5.4 mmol) (*17*). After being stirred for 2 h at room temperature, the reaction mixture was cooled to −40 °C, and mCPBA (57−86%, 1.2 g in 25 mL of CH_2Cl_2) was added. The resulting solution was stirred for 2 h at 0 °C. The reaction mixture was diluted with CH_2Cl_2 (25 mL), and the organic layer was washed with 10% aqueous Na_2SO_3 (2 × 20 mL), saturated aqueous $NaHCO_3$ (2 × 15 mL), H_2O (15 mL), and saturated aqueous NaCl (15 mL), dried (Na_2SO_4), filtered, and concentrated in vacuo. The crude product was purified by silica gel chromatography (2.5 × 5 cm, EtOAc) to give **4** (845 mg, 1.6 mmol, 89%) as a colorless oil: ^{1}H NMR ($CDCl_3$) δ 8.24 (s, 0.8 H), 8.19 (s, 0.2 H), 7.33 (m, 10 H), 6.84 (br d, J = 9.1 Hz, 1 H), 6.61 (bs, 1 H), 5.77 (dd, J = 4.3, 9.1 Hz, 0.8 H), 5.72 (d, J = 7.6 Hz, 0.2 H), 5.05 (m, 4 H), 4.63 (m, 1 H), 4.46 (m, 1 H), 4.13 (m, 1 H), 4.00 (m, 4 H), 1.51 (s, 3 H), 1.31 (s, 3 H).

The solution of **4** (845 mg, 1.6 mmol) and Pd−C (20 mg) in ethanol (100 mL) was placed in a Parr hydrogenator at 25 psi H_2. After stirring for 6 h at room temperature, the reaction mixture was filtered through Celite and concentrated to give a colorless oil. To the oil in H_2O (12 mL) was added TFA (20 μL, 0.26 mmol), and the resulting solution was stirred for 24 h at room temperature. The crude fGAR was purified by an anion exchange HPLC (SAX, 0.46 × 25 cm) to provide fGAR of maximum purity for kinetic studies. It also allowed the removal of GAR contaminant that could be formed in the last step of the synthesis. The fGAR was eluted with a linear gradient of ammonium acetate buffer (pH 7.0, 0−100 mM, 30 min) with a flow rate of 1.0 mL/min. Since fGAR did not give any detectable UV absorbance, the fGAR fractions were detected by GAR transformylase activity after they were converted to GAR by acid hydrolysis. An aliquot (90 μL) from each fraction was mixed with 10 μL of 1 N HBr, and the mixture was boiled at 100 °C for 15 min to complete the conversion (*18*). The fGAR was collected in fractions between 15 and 25 min. The undesired GAR fractions, which were eluted at 5−7 min, were detected by the enzyme assay and were well separated from fGAR fractions. The combined fGAR fractions were lyophilized to give a white powder that was dissolved in water and stored at −80 °C. The structure of fGAR was confirmed by ^{1}H NMR and mass spectrometry, identical to that reported (*16*). The concentration of β-anomer of fGAR was determined by NMR and total phosphate content by the procedure of Chen et al. (*12*).

Kinetic Measurements. Instead of the unstable natural cofactor, 10-formyltetrahydrofolate, a kinetically equivalent and more stable fDDF was used in all kinetic measurements (*4*). The initial velocity for the reaction of GAR transformylase with GAR and fDDF was determined by monitoring the production of DDF at 295 nm ($\Delta\epsilon$ = 18.9 mM^{-1} cm^{-1}). These studies were done in 1 mL cuvettes thermostated on a Gilford 252 spectrophotometer, and the reaction was initiated with one of the substrates at an enzyme concentration of 1−2 nM.

For the initial velocity of a reverse reaction in which enzyme was reacted with fGAR and DDF, the production of fDDF was monitored by a fluorescence increase at 400 nm when excited at 340 nm. The data were obtained on a stopped-flow apparatus with the enzyme concentration in the range 3−4 μM. A molar fluorescence change (ΔF) was established by measuring known concentrations of fDDF in solutions containing the same amount of enzyme and DDF used in the initial rate measurement. The molar ΔF for fDDF is only valid with a given concentration of enzyme and DDF because ΔF is different as the concentration of enzyme or DDF changes. Data were fit to the Michaelis−Menten equation to obtain k_{cat} and K_m values using a nonlinear least-squares fitting program.

Stopped-Flow Experiment. All stopped-flow experiments were performed on an Applied Photophysics Kinetic Spectrometer (Cambridge, England) that has a thermostated sample cell. The formation of fDDF in the reverse reaction and the enzyme−fDDF complex in competition experiments was monitored by excitation of the fDDF fluorescence at 340 nm with a 2 nm slit width and then by observation of the emission with an output filter at 400 nm. Enzyme−DDF complex formation was monitored by the intrinsic protein fluorescence quenching at 340 nm with excitation at 290 nm. Absorbance measurements were conducted at 295 nm with a 1 nm slit width. In most experiments, 5−8 traces were recorded and averaged for data analysis. Data were collected over a given time interval by an Archimedes computer. All data were analyzed by a nonlinear least-squares computer program provided by Applied Photophysics.

Fluorescence Titrations. The thermodynamic dissociation constants (K_d) for ligands from the enzyme or enzyme−ligand complexes were measured by fluorescence titration employing an SLM 8000 spectrofluorimeter. The binding of fDDF to the enzyme or to the enzyme−GAROH complex was followed by measuring the increase in fluorescence of fDDF at 400 nm with an excitation wavelength of 340 nm upon addition of a fDDF solution. In a control experiment, the fluorescence of fDDF in the absence of enzyme species was recorded and later used to correct the data for any background and inner filter effects. For a fluorescence titration experiment involving DDF, the quenching of the intrinsic enzyme fluorescence at 340 nm upon excitation at 290 nm was monitored as a function of ligand concentration. In this experiment, a solution of tryptophan with a fluorescence similar to that of the enzyme solution was titrated to correct for the absorbance caused by added ligands. In these experiments, the enzyme concentration used was less than $0.5K_d$, and both the excitation and emission slits were set at 4 nm. The data were fit to a quadratic equation to calculate K_d values (*19*).

Equilibrium Dialysis. The dissociation constant for GAR from GAR transformylase was measured by equilibrium dialysis. A microequilibrium dialyzer with 5 sets of chambers (25 μL in one chamber) was set up with Spectra Por 2 MWCO 12 000−14 000 dialysis tubing (*20*). An enzyme sample (63 μM) was dialyzed against a range from 200 to 600 μM of GAR while gently rotating the dialysis setup back and forth. As a control, a buffer was dialyzed against GAR to determine the time to reach equilibrium (about 4 h). The

Table 1: Steady-State Kinetic Parameters for GAR Transformylase

forward reaction		reverse reaction	
k_{cat}	$90 \pm 2\ s^{-1}$	k_{cat}	$0.73 \pm 0.02\ s^{-1}$
K_m(fDDF)	$12.3 \pm 1.3\ \mu M$	K_m(DDF)	$19.0 \pm 1.3\ \mu M$
K_m(GAR)	$118 \pm 3\ \mu M$	K_m(fGAR)	$102 \pm 5\ \mu M$

amount of GAR in each compartment was measured by enzyme turnover with 10-fold excess of fDDF.

Data Analysis. The KINSIM kinetic simulation program (*21*) was used to model the single-turnover experiments. Computer simulation of Scheme 5 was carried out with the known rate and dissociation constants. The values for the on- and off-rate of fDDF and DDF to the enzyme were estimated from the competition binding experiment. The rate constant for the interconversion step of the ternary complexes in the forward direction was set at 95 s^{-1} as measured by a single-turnover experiment, and that for the reverse direction was set at 0.7 s^{-1}, which is the steady-state k_{cat} value that represents the rate-limiting step. The dissociation constants for various species involving GAR and cofactors and the requirement of the same free-energy change for both pathways leading to the ternary complex from the free enzyme were used to constrain the fitting process. The data were fit by a trial and error process to find rate constants or equilibrium constants as the best fit to all the single-turnover results.

RESULTS AND DISCUSSION

Steady-State Kinetic Parameters. Initial velocity studies in the forward and reverse reactions gave the kinetic parameters listed in Table 1. Both the k_{cat} for the forward reaction and K_m for GAR are about 5 times higher than the previously reported values, 16 s^{-1} and 16.7 μM, respectively, measured at the same pH but in a buffer containing 50 mM Tris and 0.5 mM EDTA (*4*, *6*). The change in the buffer, however, had little effect on the parameters, so that the differing values must be due to some impurities in the GAR sample that inhibited the enzyme. In the current study, those impurities have been removed by HPLC. The measure of k_{cat} and K_m for fGAR and DDF in the reverse reaction made use of the difference in the fluorescence spectra of fDDF and DDF. A maximum difference was observed at 400 nm when excited at 340 nm. Although k_{cat} is 13-fold less, the K_m's for fGAR and DDF are not much different from those for GAR and fDDF.

Fluorescence Titrations. The binding of fDDF to GAR transformylase was measured by following the increase in fluorescence upon fDDF binding to the enzyme. The fluorescence change at 400 nm was measured as a function of fDDF concentration for fDDF alone and in the presence of enzyme. No significant primary absorption effect was observed since the increase of fluorescence at 400 nm in the absence of enzyme was linear with fDDF concentration. The corrected data were computer fit to a quadratic equation by nonlinear regression to obtain the dissociation constant of $2.5 \pm 0.4\ \mu$M. For DDF binding to GAR transformylase, the quenching of the intrinsic enzyme fluorescence upon ligand titration was followed. The data were computer fit as above to give a dissociation constant of $19 \pm 3\ \mu$M.

No noticeable change in enzyme intrinsic fluorescence was observed upon addition of GAR or fGAR at any concentration up to 0.8 mM, suggesting that GAR or fGAR does not bind to the apoenzyme. In fact, a steady-state kinetic study on murine GAR transformylase has suggested a sequential ordered mechanism in which GAR binds only to the enzyme−fDDF complex (*10*). The *E. coli* enzyme was also shown to follow a sequential type mechanism (*4*). Thus, we attempted to measure the dissociation constant for GAR from the enzyme−fDDF−GAR complex using a GAR analogue that would form a stable ternary complex. GAROH was used for this purpose because it has the same structure as the natural substrate except for a hydroxyl group instead of the amine, and has been known to act as a competitive inhibitor (*10*). Like the natural substrate, GAROH did not cause any change in the enzyme's intrinsic fluorescence. When GAROH was titrated into a solution of enzyme saturated with fDDF, there was no change in either the enzyme's intrinsic fluorescence or that of the cofactor. However, in the titration of the enzyme−DDF complex (E−DDF) with GAROH, we were able to follow the quenching of the enzyme's intrinsic fluorescence, which yielded the dissociation constant of $95 \pm 3\ \mu$M.

Scheme 3. Folate Binding Kinetics

$$\text{E-DDF} \underset{k_1}{\overset{k_{-1}}{\rightleftharpoons}} \text{E} + \text{DDF} \qquad \text{E} + \text{fDDF} \underset{k_{-2}}{\overset{k_2}{\rightleftharpoons}} \text{E-fDDF}$$

Binding of GAR to Enzyme. The fact that GAR actually binds to the apoenzyme came from an equilibrium dialysis experiment. Although it was not as accurate as using a radioactive compound, we were able to estimate the K_d as $150 \pm 40\ \mu$M employing high concentrations of enzyme. The error range is quite large because the amount of GAR was quantitated by enzyme turnover in a spectrophotometer as described in the Materials and Methods. The binding is much weaker than fDDF, and it is very close to the K_m value from the steady-state kinetics. However, it is not certain from this experiment alone whether GAR binding actually leads to a productive ternary complex.

Cofactor Binding Kinetics. Because the binding of fDDF or DDF with GAR transformylase induces a change in fluorescence, the measurement of on- and off-rate for cofactor binding was attempted by following an appropriate fluorescence signal resulting from mixing enzyme with cofactor. Unfortunately, no fluorescence change was detected in the formation of a binary complex using stopped-flow mixing of 0.5−7 μM enzyme and 50−100 μM fDDF or DDF (final concentration). Either the rate of approach to equilibrium is so fast that most of the signal is lost during the dead time of the stopped flow, or the signal itself may be too small to be detected because, in the titiration of fDDF to the enzyme, the total change of signal represented only about 3%.

Next, we tried a competition experiment in which the enzyme−DDF complex was mixed with fDDF that competes for the folate binding site (Scheme 3). The formation of the enzyme−fDDF complex (E−fDDF) was followed by a time-dependent increase in the fluorescence signal at 400 nm (Figure 1). The observed rate constant can be expressed in terms of the rate constants in Scheme 3 under the near-equilibrium condition (*22*), and is a function of all four rate constants and the concentration of DDF and fDDF (eq 1).[3]

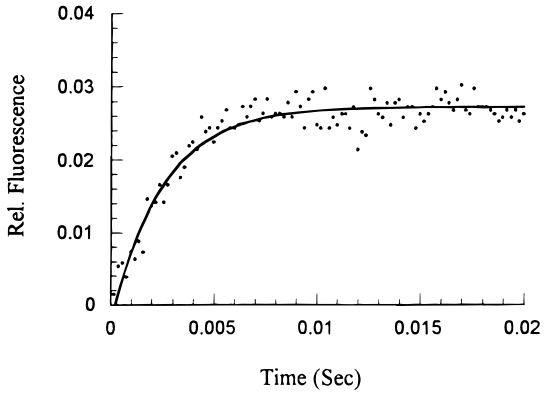

FIGURE 1: Competition experiment for cofactor binding. E−DDF binary complex (68 μM DDF, 7 μM GAR transformylase) was mixed with fDDF (39 μM) (concentrations after mixing) and the fluorescence increase monitored at 400 nm resulting from the formation of the E−fDDF complex in MTEN buffer, pH 7.5, 25 °C. The data were fit to a first-order rate equation.

$$k_{obs} = \frac{k_{-1}(k_{-2} + k_2[\text{fDDF}]) + k_1[\text{DDF}]k_{-2}}{k_{-1} + k_1[\text{DDF}] + k_2[\text{fDDF}] + k_{-2}} \quad (1)$$

$$K_d(\text{DDF}) = \frac{k_{-1}}{k_1}, \quad K_d(\text{fDDF}) = \frac{k_{-2}}{k_2} \quad (2)$$

By varying the DDF concentration between 34 and 135 μM and fDDF between 39 and 230 μM, we obtained k_{obs} values ranging from 380 to 670 s^{-1}. These k_{obs} values were then fit to eq 1 by using a nonlinear regression curve fitting in the SIGMAPLOT program (v. 4.14 for Macintosh). By reducing the number of parameters (individual rate constants) 2-fold by substituting the known values of K_d for DDF and fDDF (eq 2), the resulting rate constants were $k_1 = (4.0 \pm 0.5) \times 10^7$ M^{-1} s^{-1}, $k_{-1} = 772 \pm 123$ s^{-1}, $k_2 = (5.5 \pm 1.0) \times 10^7$ M^{-1} s^{-1}, and $k_{-2} = 143 \pm 32$ s^{-1}. The dissociation rate constants for fDDF and DDF are much higher than the steady-state k_{cat} value for the forward and reverse reactions, indicating that the dissociation of the cofactors from the binary complexes is not rate-limiting during steady-state turnover.

Pre-Steady-State Experiments. No pre-steady-state transient was observed in either direction by stopped-flow methods using up to 7 μM enzyme and saturating concentrations of substrates. No rapid reaction occurred during the dead time of the instrument because the curve extrapolated to the point of $\Delta A = 0$ or $\Delta F = 0$. No pre-steady-state transient was observed at pHs ranging from 6 to 10 in either direction. Thus, it is likely that the rate-determining step during steady-state turnover is a step involving the ternary complexes.

Single-Turnover Experiments of the Forward Reaction. Since the above experiments implied that the catalytic step itself may be rate-limiting, we investigated more closely the chemistry step at the enzyme active site using enzyme in excess of substrate, so that the conversion of substrates to products is complete in a single turnover of the enzyme. Both free enzyme and binary complexes were subjected to various

[3] Actually, the fluorescence change should be a double exponential with another rate constant, $1/\tau = k_{-1} + k_1[\text{DDF}] + k_2[\text{fDDF}] + k_{-2}$. However, this rate is too fast to be measured and therefore is not considered in the fitting.

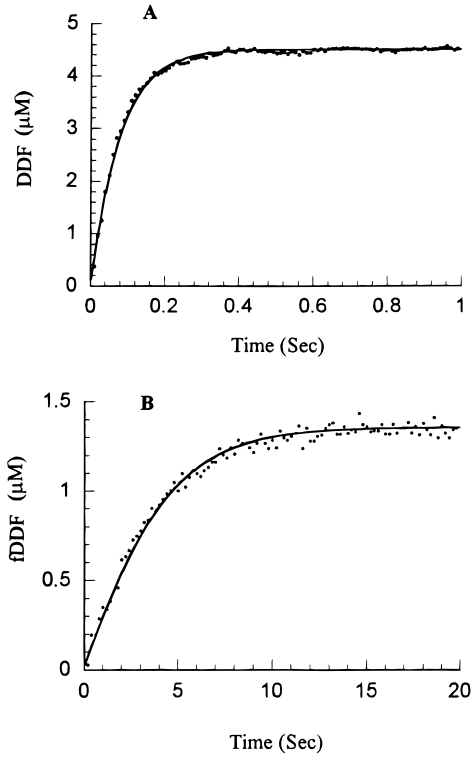

FIGURE 2: Time course for a single-turnover reaction. (A) Forward reaction. E−fDDF complex (124 μM fDDF, 14 μM GAR transformylase) was mixed with GAR (4.7 μM) (concentrations after mixing), and the formation of DDF was monitored. (B) Reverse reaction. E−DDF complex (667 μM DDF, 14 μM GAR transformylase) was mixed with fGAR (5.2 μM) (concentrations after mixing), and the formation of fDDF was monitored by fluorescence increase at 400 nm. The data were simulated with the kinetic parameters listed in Scheme 5.

single-turnover conditions with a given substrate in limiting concentration. Representative plots from single turnover in either direction are shown in Figure 2. The data were fit to single exponentials and k_{obs} values were obtained. Table 2 summarizes the various single-turnover experiment results in either direction.

The first of such experiments has enzyme preincubated with fDDF and the reaction initiated by mixing of GAR with the production of DDF monitored at 295 nm (reactions 1 and 2). When fDDF was at a limiting concentration (reaction 2), the value of k_{obs} was very close to k_{cat} for the steady-state experiment and was independent of protein concentration, demonstrating that the binding of fDDF to the enzyme active site was not rate-limiting. This strongly suggests that the rate-limiting step during steady-state turnover involves the ternary complexes, E−fDDF−GAR and E−DDF−fGAR. Thus, the catalytic efficiency, k_{cat}/K_m for fDDF, which is 7.5×10^6 M^{-1} s^{-1}, reflects an interconversion step, not the rate of binding of fDDF. When GAR was at a limiting concentration (reaction 1), a much lower k_{obs} (13 s^{-1}) was obtained. This rate constant showed a linear dependence on protein concentration, suggesting that the binding of GAR to the binary complex is rate-limiting under the condition of reaction 1.

Single-turnover experiments were also performed with two different preincubation conditions as shown in reaction pairs 3 and 4 or 5 and 6. Interestingly, different rate constants were obtained depending on the preincubation and mixing

Table 2: Single-Turnover Reactions[a]

reaction no.	foward reaction						reverse reation					
	E	+	fDDF	→	GAR	k_{obs} (s^{-1})	E	+	DDF	←	fGAR	k_{obs} (s^{-1})
1	14		124		4.7	13.2 ± 0.6	14		667		5.2	0.23 ± 0.03
2	14		2.5		470	93.6 ± 1.0	14		5.3		520	0.53 ± 0.04
	E	+	GAR	→	fDDF		E	+	fGAR	←	DDF	
3	14		4.7		124	7.1 ± 1.4	14		5.2		667	0.13 ± 0.02
4	14		470		2.5	95.0 ± 3.9	14		520		5.3	0.66 ± 0.05
	E	→	fDDF	+	GAR		E	←	DDF	+	fGAR	
5	14		124		4.7	6.8 ± 1.5	14		667		5.2	0.12 ± 0.02
6	14		2.5		470	78.5 ± 5.5	14		5.3		520	0.45 ± 0.02

[a] Concentrations of E, fDDF, GAR, DDF and fGAR are given in μM.

Scheme 4. Possible Kinetic Mechanism for Single Turnover Reactions

A. Ordered Mechanism

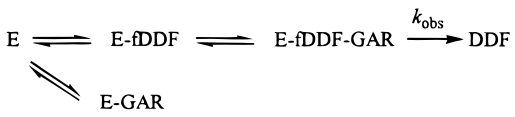

B. Random Mechanism

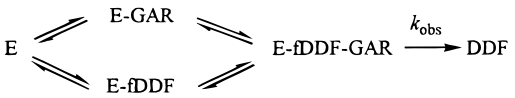

condition, although the same concentration of substrate and enzyme was used in each reaction pair. These experiments provide a good assessment of the importance of kinetic ordering of substrates. Since GAR binds to the apoenzyme, the question is whether the E−GAR complex can proceed directly to a productive ternary complex. Scheme 4 shows two possible sequential kinetic mechanisms, ordered and random. Reactions 1 and 2 do not distinguish between the ordered and the random mechanisms because most of the enzyme is in the form of the enzyme−fDDF complex (E−fDDF) during preincubation and the reactions will follow the same pathway in both mechanisms (Scheme 4).

In reaction 4, most of the enzyme is in the form of the E−GAR complex in the preincubation mixture. The reaction proceeded with the same k_{obs} as reaction 2, indicating that an identical level of productive ternary complex was formed directly from the E−GAR complex. This result clearly shows that the reaction follows a random sequential kinetic mechanism. Likewise, owing to random binding, the condition for reaction 3 is identical to that for reaction 5 as verified by similar k_{obs} values. Although reactions 3 and 5 are comparable to reaction 1, the latter k_{obs} is 50% higher. To explain this difference as well as the k_{obs} value for reaction 6, we introduced a second E−fDDF complex. In reaction 6, both pathways in the random mechanism become equally important even though GAR is in large excess over fDDF because of the lower affinity of GAR for the apoenzyme. However, if the initial E−fDDF complex has to further isomerize to a second E−fDDF complex, a decrease in the overall k_{obs} would result. The random action of the pathway is supported by the fact that the k_{obs} for reaction 6 was increased when a higher concentration of GAR was used. Collectively, the single-turnover experiments are consistent with the minimal kinetic mechanism in the forward direction presented in Scheme 5.

The physical nature of the isomerization step is currently unknown. Crystallographic results, however, have indicated a conformational change upon binding of fDDF to the enzyme. A flexible loop consisting of amino acids 110−132 has a disordered structure in the apoenzyme and becomes better resolved with folate bound to it (*8, 9*). Mutagenesis studies also have implicated this loop in folate binding (*6*).

Single-Turnover Experiments of the Reverse Reaction. Single-turnover kinetics in the reverse direction were measured by the increase in fluorescence at 400 nm as fDDF formed. A sequence of single-turnover experiments identical to that in the forward direction was performed (Table 2 and Figure 2). The observed rate constants were in the range from 0.1 to 0.7 s^{-1}, about 100 times lower in value than the corresponding k_{obs} from the forward reactions. However, it appeared that the reverse reactions did not go to completion, converting only ~25% of the substrate to the product (Figure 2B), indicating that the k_{obs} values represent the rate of reaching equilibrium. Interestingly, their relative values are very similar to those in the forward reaction. Since the concentrations of limiting substrate were the same in each set of reactions, the differences in these rate constants must be due to the order of binding and mixing. Thus, the same course of reasoning as in the forward reactions was used to establish the minimal kinetic scheme for the reverse reaction. However, the k_{obs} value from reaction 2 was lower than that from reaction 4. This is due to a weak binding of DDF to the enzyme, resulting in less than half of DDF being bound to the enzyme in the preincubation of reaction 2, suggesting that DDF binds more tightly to the E−fGAR complex. This is the case because the dissociation constant of DDF from E−DDF−fGAR complex is 10 μM but 20 μM from E−DDF complex (vide infra). The smaller k_{obs} for reactions 3 and 5 compared to reaction 1 where the levels of ligands are identical also is consistent with the isomerization of the initial E−DDF complex as in the lower k_{obs} found in reaction 6 relative to reaction 2.

The steady-state k_{cat} value is the same order of magnitude as the k_{obs} values, indicating that the interconversion of the ternary complexes is the rate-limiting step during steady-state turnover in the reverse direction.

Binding of Cofactor to E−GAR. The equilibrium constant for binding of fDDF to E−GAR was estimated by using GAROH. The fluorescence change of fDDF at 400 nm was monitored upon addition to enzyme saturated with GAROH. After subtraction of fluorescence due to fDDF alone, the data were fit to the quadratic equation to give a dissociation constant of 1.2 ± 0.3 μM. Attempts to measure the on- and

Scheme 5. Kinetic Scheme for GAR Transformylse at 25 °C in MTEN Buffer, pH 7.5

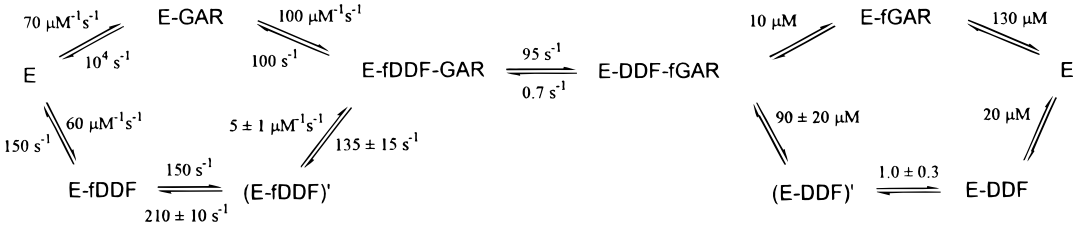

off-rate of fDDF to enzyme−GAROH complex in a stopped-flow experiment were not successful. The binding of DDF to enzyme−GAROH was also measured by monitoring the quenching of intrinsic protein fluorescence upon addition of DDF. Fitting the data to a quadratic equation gave a dissociation constant of 9.8 ± 0.9 μM.

Computer Simulation of Kinetic Constants. Based on the proposed mechanism in Scheme 5, the single-turnover results were simulated by using the KINSIM simulation program as described in Materials and Methods. The simulated rate or equilibrium constants are summarized in Scheme 5. The reverse reactions were equilibrium processes and we assumed that the E−fDDF and E−fDDF−GAR complexes had identical spectroscopic properties. This assumption is reasonable since there was no change in ΔF upon binding of GAROH to the E−fDDF complex. In the simulation of reverse reactions, we were only able to estimate the equilibrium constant for each step. For the forward reactions, however, only one set of rate constants gave a best fit and satisfied a closed thermodynamic cycle comprised of both pathways leading to the ternary complex.

Summary of Overall Kinetic Scheme. The *E. coli* GAR transformylase follows a random sequential mechanism. Single-turnover experiments showed that the enzyme can bind GAR productively, which was confirmed by equilibrium binding measurements. Interestingly, a recent study of mouse GAR transformylase has also suggested a random order of substrate binding (*23*), contrary to the originally proposed ordered binding. The fact that the enzyme can bind GAR productively seems reasonable when considering potential substrate channeling between the purine biosynthetic enzymes (*24*). GAR transformylase is found in vertebrates in the form of a multifunctional enzyme (*24*). Although *E. coli* GAR transformylase is purified as a monomer, it is conceivable that the purine pathway enzymes in *E. coli* also form a multienzyme complex for efficient substrate channeling. For such channeling it is advantageous to have an enzyme−GAR complex.

The kinetic constants show that fDDF has a higher affinity for the apoenzyme than GAR does. However, the natural cofactor, 10-formyltetrahydrofolate, may not bind the enzyme as tightly as fDDF because its K_m is about 5 times higher than that for fDDF at pH 7.5 (*4*). The small difference in the enzyme's binding capability between folate and GAR is inconsequential because the rate-limiting step in the steady-state turnover in either direction (k_{cat}) is the interconversion step of the ternary complexes. This is further supported by the measurement of a solvent isotope effect on k_{cat}. A preliminary experiment showed a pL-independent (L = H or D) solvent deuterium isotope effect of about 2 for k_{cat} in each direction (Shim, J. H., and Benkovic, S. J., unpublished results). A potential role for a water molecule in the proton transfer between the amino group of glycine and N10 of the cofactor during catalysis has been postulated on the basis of mutagenesis studies guided by the crystal structure (*6*). The collection of kinetic and equilibrium constants in Scheme 5 should be sufficient to provide a basis for understanding the effect of mutations on the catalytic cycle of GAR transformylase.

REFERENCES

1. Marolewski, A., Smith, J. M., and Benkovic, S. J. (1994) *Biochemistry 33*, 2531−2537.
2. Nygaard, P., and Smith, J. M. (1993) *J. Bacteriol. 175*, 3591−3597.
3. Smith, J. M., and Daum, H. A., III (1987) *J. Biol. Chem. 262*, 10565−10569.
4. Inglese, J., Johnson, D. L., Shiau, A., Smith, J. M., and Benkovic, S. J. (1990) *Biochemistry 29*, 1436−1443.
5. Daubner, S. C., Young, M., Sammons, R. D., Courtney, L. F., and Benkovic, S. J. (1986) *Biochemistry 25*, 2951−2957.
6. Warren, M. S., Marolewski, A., and Benkovic, S. J. (1996) *Biochemistry 35*, 8855−8862.
7. Chen, P., Schulze-Gahmen, U., Stura, E. A., Inglese, J., Johnson, D. L., Marolewski, A., Benkovic, S. J., and Wilson, I. A. (1992) *J. Mol. Biol. 227*, 283−292.
8. Almassy, R. J., Janson, C. A., Kan, C.-C., and Hostomska, Z. (1992) *Proc. Natl. Acad. Sci. U.S.A. 89*, 6114−6118.
9. Klein, C., Chen, P., Arevalo, J. H., Stura, E. A., Marolewski, A., Warren, M. S., Benkovic, S. J., and Wilson, I. A. (1995) *J. Mol. Biol. 249*, 153−175.
10. Caperelli, C. A. (1989) *J. Biol. Chem. 264*, 5053−5057.
11. Sheehan, J. C., and Yang, D.-D. H. (1958) *J. Am. Chem. Soc. 80*, 1154−1158.
12. Chen, P. S., Toribara, T. Y., and Warner, H. (1956) *Anal. Chem. 28*, 1756−1758.
13. Inglese, J., Blatchly, R. A., and Benkovic, S. J. (1989) *J. Med. Chem. 32*, 937−940.
14. Boschelli, D. H., Powell, D., Sharky, V., and Semmelhack, M. F. (1989) *Tetraheron Lett. 30*, 1599−1600.
15. Chettur, G., and Benkovic, S. J. (1977) *Carbohydr. Res. 56*, 75−86.
16. Schendel, F. J., and Stubbe, J. (1986) *Biochemistry 25*, 2256−2264.
17. Yu, K.-L., and Fraser-Reid, B. (1988) *Tetrahedron Lett. 29*, 979−982.
18. Warren, L., and Buchanan, J. M. (1957) *J. Biol. Chem. 229*, 613−626.
19. Taira, K., and Benkovic, S. J. (1988) *J. Med. Chem. 31*, 129−137.
20. Washburn, W. K. (1984) M.S. Thesis, The Pennsylvania State University.
21. Barshop, B. A., Wrenn, R. F., and Frieden, C. (1983) *Anal. Biochem. 130*, 134−145.
22. Hammes, G., and Schimmel, P. R. (1970) *Enzymes, 3rd Ed. 2*, 67−114.
23. Sanghani, S. P., and Moran, R. G. (1997) *Biochemistry 36*, 10506−10516.
24. Zalkin, H., and Dixon, J. E. (1992) *Prog. Nucleic Acid Res. Mol. Biol. 42*, 259−287.

BI980244K